PROTEINS
STRUCTURE ■ FUNCTION ■ BIOINFORMATICS

What stabilizes the 3_{14}-helix in β^3-peptides? A conformational analysis using molecular simulation

Bettina Keller,[1]* Zrinka Gattin,[2] and Wilfred F. van Gunsteren[1]

[1] Laboratory of Physical Chemistry, Swiss Federal Institute of Technology Zürich, ETH Zürich, CH-8093 Zürich, Switzerland
[2] Max Planck Institute for Biophysical Chemistry, Research Group Solid-state NMR, Am Faßberg 11, D-37077 Göttingen, Germany

ABSTRACT

β-Peptides are analogs of natural α-peptides and form a variety of remarkably stable structures. Having an additional carbon atom in the backbone of each residue, their folded conformation is not only influenced by the side-chain sequence but also and foremost by their substitution pattern. The precise mechanism by which the side chains interact with the backbone is, however, hitherto not completely known. To unravel the various effects by which the side chains influence the backbone conformation, we quantify to which extent the dihedral angles of a β^3-substited peptide with an additional methyl group on the central C_α-atom can be regarded as independent degrees of freedom and analyze the distributions of these dihedral angles. We also selectively capture the steric effect of substituents on the C_α- and C_β-atoms of the central residue by alchemically changing them into dummy atoms, which have no nonbonded interactions. We find that the folded state of the β^3-peptide is primarily stabilized by a steric exclusion of large parts of the unfolded state (entropic effect) and only subsequently by mutual dependence of the ψ-dihedral angles (enthalpic effect). The folded state of β-peptides is stabilized by a different mechanism than that of α-peptides.

Proteins 2010; 78:1677–1690.

Key words: β-peptides; peptide folding; molecular dynamics; conformational analysis; mutual information.

INTRODUCTION

β-Peptides

β-Peptides are mimetics of natural α-peptides and a remarkable class of nonnatural polypeptides. They exhibit a large variety of folded structures, among which are several types of helices, and they typically fold on timescales, which are faster than those of their natural analogs, the α-peptides. Furthermore, other than α-peptides, they already form stable secondary structures with very short chain lengths. Two aspects of these foldamers fuel the interest of the scientific community: (i) their resistance to proteases combined with their ability to form secondary structures, which parallel those of natural peptides make them promising candidates for rationally designed drugs[1] and (ii) their short folding time scales permit extensive molecular dynamics studies of the folding process making them an ideal test case for the investigation of peptide folding.[2]

The peptide planes in β-peptides are separated by two carbon atoms thereby offering an additional site for altering substitution sequence and substitution pattern, which ultimately determine the secondary structure. Much is known already about the relation between the molecular composition and structural preferences of β-peptides. In this study, we examine β-heptapeptides, which fold into 3_{14}-helices (Fig. 1), and therefore, only list current knowledge that is relevant to formation of these helices.

- The substitution pattern has more influence on the folding equilibrium than the sequence of the substituents.[3,4]
- Substituents, which occupy the C^{Si}-position, both on C_α and C_β, are lateral, that is, the central bonds of their χ_1 dihedral angles are perpendicular to the axis of the 3_{14}-helix. They do not sterically hinder the helix-formation. If, on the other hand, the substituents occupy the C^{Re}-position, they end up in an axial position and due to steric hindrance break the helix.[5]
- Peptides consisting of amino acids with C^{Si}-configured substituents on the C_β-atom (β^3-peptides) form particularly stable 3_{14}-helices.[3,6] Obviously, substituents in these positions do more than simply not disturbing the he-

Additional Supporting Information may be found in the online version of this article.
*Correspondence to: Bettina Keller, Laboratory of Physical Chemistry, ETH Hönggerberg, HCI, CH-8093 Zürich.
E-mail: bettina@igc.phys.chem.ethz.ch
Received 13 August 2009; Revised 20 October 2009; Accepted 14 November 2009
Published online 14 January 2010 in Wiley InterScience (www.interscience.wiley.com).
DOI: 10.1002/prot.22685

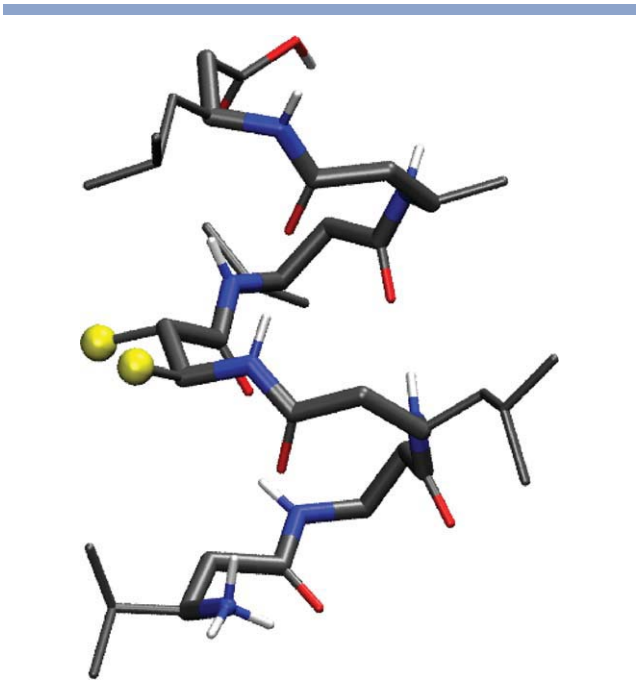

Figure 1

3_{14}-helical conformation of peptide A. The methyl groups on residue 4 which are perturbed to dummy atoms in peptide B–D are highlighted in yellow.

lix formation - they actively promote it. If the substituents are additionally branched at the first carbon atom, they stabilize the helix even more.[6] It has been argued that a substituent on the C_β-atom sterically hinders variation of the ϕ-dihedral angle thereby decreasing its accessible conformational space.[3,6]

- β^3-peptides, which have an additional C^{Si}-configured substituent on the C_α of their central residue, have been shown by NMR[5] and MD simulations[7] to possess increased 3_{14}-helix propensity.
- The θ-backbone dihedral angle is found to be restricted to either ≈60° or ≈180° in most of the known β-peptides, and therefore, is often not considered to be a flexible degree of freedom.[3]
- The helix propensities of β^3-amino acids differ strongly from those of natural α-amino acids.[6]

Although these facts are well-established for several years now, the precise mechanism by which the substituents stabilize the helix is hitherto unknown. The present study is based on extensive molecular dynamics simulations of β-heptapeptides in explicit solvent, which have been shown to be in agreement with the available NMR-data. In each simulation of β-peptides, which fold into a 3_{14}-helix, we observe several folding and unfolding events. To unravel the various effects by which the side chains influence the backbone conformation, we quantify to which extent the dihedral angles can be regarded as independent degrees of freedom and analyze the distributions of these dihedral angles. We also selectively capture the steric effect of substituents on the C_α- and C_β-atoms by alchemically changing them into dummy atoms, which have no nonbonded interactions.

In this contribution, the term configuration denotes the chemical configuration, that is, the spatial arrangement of bonds in a molecule while neglecting rotation around single bonds. The term conformation denotes the spatial arrangement of atoms in a molecule of a given (chemical) configuration, that is, different conformations can be transformed into each other by rotation around single bonds. The term structure is used interchangeably with the term conformation.

METHODS

Simulation

As reported previously,[8] MD simulations of the β-heptapeptide H_2^+-β-HVal-β-HAla-β-HLeu-(*S,S*)-β-HAla(αMe)-β-HVal-β-HAla-β-HLeu-OH (see structure A in Fig. 2) in methanol were performed. The methanol solvent molecules were represented using a rigid three-site model belonging to the standard GROMOS96 set of solvents.[9] Aliphatic CH_n groups of the solute and the solvent were treated as united atoms.[10] The β-heptapeptides were protonated at the C- and N-termini yielding a positive charge of +1e. No counter-ions were used. The starting structures for each of the separate simulations (replicas) were taken randomly from a previous simulation[11] of 400 ns. Each of the 20 separate simulations (replicas) was simulated for 500 ns, adding up to a total of 10 μs of simulation data. The simulations were carried out with the GROMOS96 software[9,12] and the GROMOS 43A1 force field[9] as described previously.[11] All bond lengths were constrained using the SHAKE algorithm[13] with a relative geometric tolerance of 10^{-4} allowing for a time step of 2 fs. Solute structures were saved every 0.1 ps. The system was simulated in a rectangular box using periodic boundary conditions. The volume was kept constant and the solvent and solute molecules were independently weakly coupled to temperature baths of 310 K[14] with a coupling time of 0.1 ps. The number of solvent molecules was 962. Long-range interactions were handled using a triple-range cut off scheme[9,12] with cut off radii of 0.8 nm (interactions updated every timestep) and 1.4 nm (interactions updated every five timesteps). The mean effect of omitted electrostatic interactions beyond the long-range cut off distance (1.4 nm) was accounted for by the inclusion of a Barker–Watts reaction-field force[15,16] based on a dielectric permittivity of $\varepsilon_{rf} = 1.0$, as was done in an earlier simulation by Daura *et. al.*[7]

Starting from the simulation of peptide A, we performed three independent simulations in which peptide A was modified or perturbed: (i) the methyl-group on the C_α-atom of residue 4 (peptide B), (ii) the methyl-group on the C_β-atom of residue 4 (peptide C), and (iii)

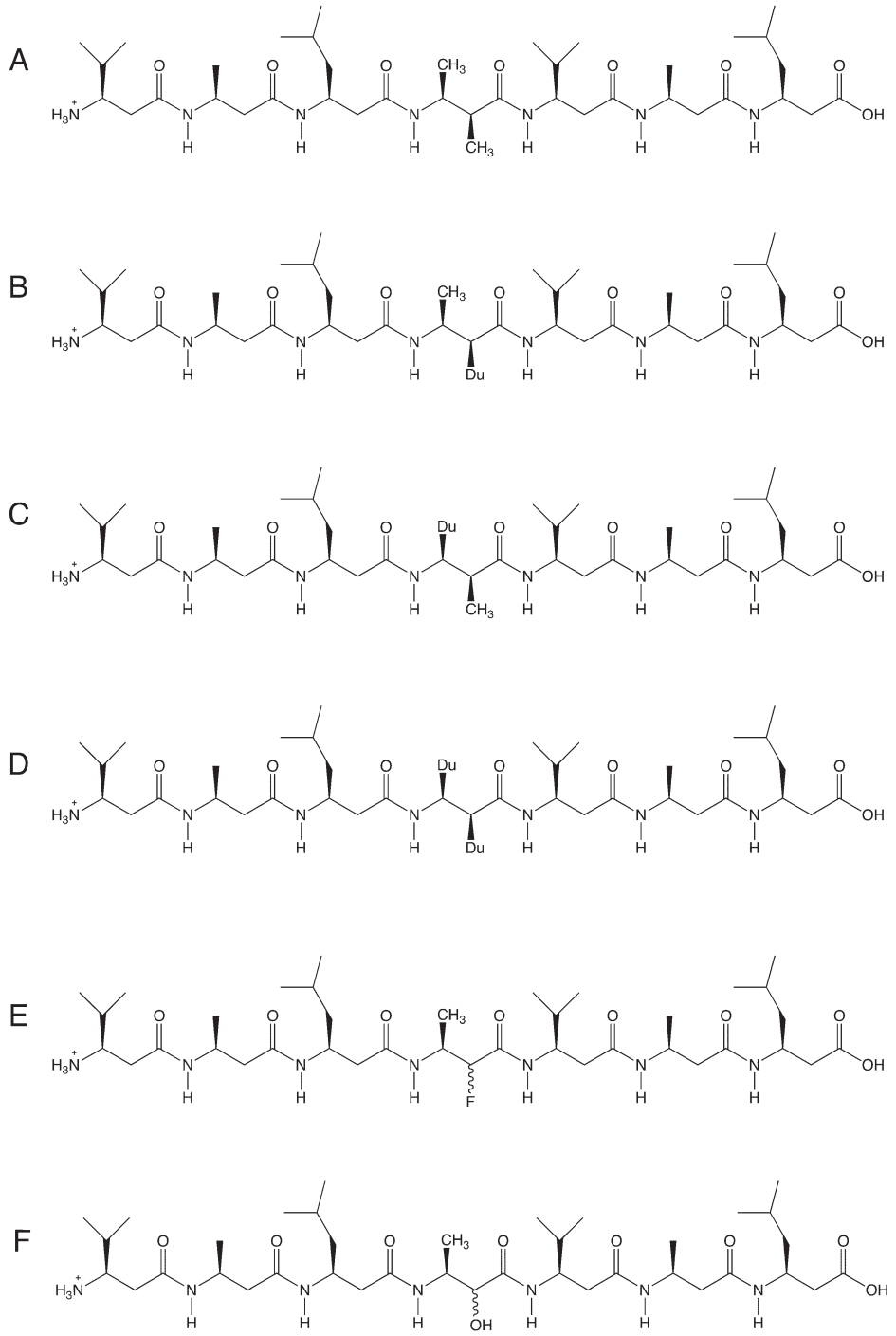

Figure 2

Chemical formula of β-heptapaptides of the form H_2^+-β-HVal-β-HAla-β-HLeu-X-β-HVal-β-HAla-β-HLeu-OH, panel A: X=(*S*,*S*)-β-HAla(αMe) (peptide **1**); panel B: X=(*S*,*S*)-β-HAla(αDu) (peptide **1a**); panel C: X=(*S*,*S*)-β-HDu(αMe) (peptide **1b**); panel D: X=(*S*,*S*)-β-HDu(αDu) (peptide **1c**); panel E: X=(*S*,*S*)-β-HAla(αF) (peptide **2**), and X=(*S*,*R*)-β-HAla(αF) (peptide **3**), resp., panel F: X=(*S*,*S*)-β-HAla(αOH) (peptide **4**), and X=(*S*,*R*)-β-HAla(αOH) (peptide **5**), resp. Du = dummy atom.

both methyl-groups on residue 4 (peptide D) were perturbed into dummy atoms, that is, atoms without nonbonded interactions. The degree of perturbation depended on a parameter λ in the Hamiltonian such that for λ = 0 the perturbed methyl group had its full nonbonded interaction, while for λ = 1 this interaction was zero.[12] To exclusively capture the steric effect of the methyl groups, we gradually disappeared the nonbonded

Table I
Summary of the Performed Simulations

	Residue 4	λ	*T*/*K*	Force field	Resolution	No. of replicas	Sim. length	Total sim. time
Peptide A	*(S,S)*Ala(αMe)	0.00	310	43A1	0.1 ps	20	500 ns	10 μs
		0.25	310	43A1	1 ps	5	50 ns	0.25 μs
		0.50	310	43A1	1 ps	5	50 ns	0.25 μs
		0.75	310	43A1	1 ps	5	50 ns	0.25 μs
Peptide B	*(S,S)*Ala(αDum)	1.00	310	43A1	1 ps	5	100 ns	0.50 μs
		0.25	310	43A1	1 ps	5	50 ns	0.25 μs
		0.50	310	43A1	1 ps	5	50 ns	0.25 μs
		0.75	310	43A1	1 ps	5	50 ns	0.25 μs
Peptide C	*(S,S)*Dum(αMe)	1.00	310	43A1	1 ps	5	100 ns	0.50 μs
		0.25	310	43A1	1 ps	5	50 ns	0.25 μs
		0.50	310	43A1	1 ps	5	50 ns	0.25 μs
		0.75	310	43A1	1 ps	5	50 ns	0.25 μs
Peptide D	*(S,S)*Dum(αDum)	1.00	310	43A1	1 ps	5	100 ns	0.50 μs
Peptide E	*(S,S)*Ala(αF)	–	340	45A3	1 ps	5	100 ns	0.50 μs
Peptide E	*(S,R)*Ala(αF)	–	340	45A3	1 ps	1	100 ns	100 ns
Peptide F	*(S,S)*Ala(αOH)	–	340	45A3	1 ps	5	100 ns	0.50 μs
Peptide F	*(S,R)*Ala(αOH)	–	340	45A3	1 ps	1	100 ns	100 ns

interaction of the united-atom-CH_3-groups using a soft-core interaction function,[17] but left the bond-, bond-angle, and dihedral angle energy terms involving this united atom unchanged. Analogously to the thermodynamic integration technique, we performed simulations at distinct λ-values: 0.25, 0.50, 0.75, 1.00 for each of the perturbations. For each λ-value, we generated five trajectories of 50 ns (λ = 0.25, 0.50, 0.75) or 100 ns (λ = 1.00) length, adding up to a total simulation time of 250 ns and 500 ns, respectively. The starting structures were drawn from the simulation of peptide A and equilibrated for 1 ns. All other simulation parameters were as in the simulations of peptide A.

The simulations of the β-heptapeptides E (residue 4 = (*S,S*)-β-HAla(αF) and residue 4 = (*S,R*)-β-HAla(αF)) and F (residue 4 = (*S,S*)-β-HAla(αOH) and residue 4 = (*S,R*)-β-HAla(αOH)) in Figure 2 were carried out in explicit solvent methanol using the GROMOS05 biomolecular simulation software[18] and force-field parameter set 45A3.[19] The solute and the solvent were modeled analogously to the simulations of peptide A in Figure 2. The solute and solvent temperatures were maintained independently at 340 K by weak coupling to two temperature baths with relaxation times of 0.1 ps.[14] The pressure was calculated using a molecular virial and maintained by weak coupling to a pressure bath (isotropic coordinate scaling) with a relaxation time of 0.5 ps, using an isothermal compressibility of $4.575 \cdot 10^{-4}$ $(\mathrm{kJmol^{-1}\ nm^{-3}})^{-1}$. We used a dielectric permittivity ε_{rf} = 19.0 of methanol[20] beyond the long-range cut off distance (1.4 nm) as in Ref. 21, 22. All other simulation parameters were equal to those of the simulations of peptide A. The simulations of *(S,R)*-configured peptides were 100 ns in length and have been reported previously.[21,22] For the *(S,S)*-configured structures we generated in both cases four trajectories of 100 ns additionally to the 100 ns-trajectories that were reported in Ref. 21, 22, adding up to a total simulation time of 0.50 μs. The initial coordinates for these additional simulations were randomly extracted from the latter 100 ns-trajectories. The analysis was based on configurations saved every 1 ps.

All simulations analyzed in this study are summarized in Table I.

Normalized mutual information and informational entropy

The problem of analyzing the folding behavior of a peptide is equivalent to analyzing the probability density p of finding the molecule in a given conformation. Although p is in principle, a function of all degrees of freedom in the system, the solute dihedral angles are usually sufficiently decoupled from the other solute degrees of freedom, such that p can be safely approximated as a function of the solute dihedral angles ν_i (with $i \in n$ and n being the number of dihedral angles in the solute molecule)

$$p = p(\nu_1, \nu_2, \ldots \nu_n), \tag{1}$$

that is, the folding can be described in terms of the dihedral angles. Except for the simplest cases (two or three dihedral angles) this function is too complex to be interpreted directly. One way to reduce the complexity of the function is by analyzing the mutual dependence between pairs of dihedral angles $\{\nu_i, \nu_j\}$. If the marginal distribution of ν_i, $p_i(\nu_i)$, does not depend on the value of ν_j and vice versa, then the mutual dependence is low and the total distribution can be approximated as the product of the marginal distributions

$$p_{ij}(\nu_i, \nu_j) \approx p_i(\nu_i) \cdot p_j(\nu_j). \tag{2}$$

Here, the term marginal distribution denotes the projection of the complete distribution $p_{ij}(\nu_i, \nu_j)$ onto one of its degrees of freedom, for example,

$$p_i(\nu_i) = \int_{\nu_j} p_{ij}(\nu_i, \nu_j) d\nu_j \quad (3)$$

One measure for mutual dependence is the mutual information MI

$$\mathrm{MI}(\nu_i, \nu_j) = \int_{\nu_i} \int_{\nu_j} p_{ij}(\nu_i, \nu_j) \log\left(\frac{p_{ij}(\nu_i, \nu_j)}{p_i(\nu_i) p_j(\nu_j)}\right) d\nu_i\, d\nu_j. \quad (4)$$

The values of MI are not confined to a certain interval. Therefore, in practice, one uses the normalized mutual information NMI, which is confined to [0,1], with NMI = 0 corresponding to absence of mutual dependence. The normalized mutual information is given as

$$\mathrm{NMI}(\nu_i, \nu_j) = \frac{\mathrm{MI}(\nu_i, \nu_j)}{\min(H_i, H_j)} \quad (5)$$

where H_i is the informational entropy of the marginal probability density $p_i(\nu_i)$

$$H_i = -\int_{\nu_i} p_i(\nu_i) \log p_i(\nu_i) d\nu_i. \quad (6)$$

Typically, one considers two dihedral angles to be mutually independent if their NMI is lower than 0.1.[8,23]

For the calculation of the normalized mutual information of dihedral angle pairs, we extracted structures at an interval of 1 ps from all replicas leading to a data set of 10,000,000 structures for β-heptapeptide A and data sets of 500,000 structures for β-heptapeptides B–F. The normalized mutual information NMI was calculated for all dihedral angle pairs using the discretized version of Eq. 5 with a grid spacing along each dihedral angle of 1°. Analogously, the informational entropy H was calculated using the discretized version of Eq. 6 with the same grid spacing.

Dihedral-angle distributions and conditional dihedral-angle distributions

For the dihedral angle distributions of β-heptapeptide A, we extracted structures at an interval of 10 ps from all 20 replicas. For those of β-heptapeptides E and F and for those of the perturbations to β-heptapeptides B–D, we extracted structures at an interval of 1 ps from all replicas. The conditional distributions were constructed (i) by deleting from the data sets the structures for which ψ_4 lies in the interval [180,240] to obtain the set "ψ_4 not in maximum III" (see Fig. 4) and (ii) by deleting from these data sets the structures for which ψ_4 does not lie in the interval [180,240] to obtain the set "ψ_4 in maximum III."

Hydrogen-bond analysis

The hydrogen-bond analysis uses as criterion for defining a hydrogen bond, a maximum hydrogen-acceptor distance of 0.25 nm, and a minimum donor atom-hydrogen acceptor angle of 135°. It was performed on 500,000 structures of β-heptapeptide A (structures extracted every 1 ps from replica 7), on 250,000 structures for each of the λ-values for the perturbations to the "virtual" β-heptapetides B, C, and D (structures extracted every 1 ps from replicas 1 to 5), and on 500,000 structures of the *(S,S)*-substituted peptides E and F (structures extracted every 1 ps from all replicas).

Geometric cluster analysis

For the geometric cluster analysis, we extracted 15,000 structures at intervals of 100 ps from the simulations of peptide A, 25,000 structures at intervals of 10 ps from each of the perturbation simulations to peptides B–C, 16,500 structures at intervals of 30 ps from the simulations of peptide E (residue 4 = (*S,S*)H-Ala(αF)) and 14,433 structures at intervals of 30 ps from the simulations of peptide F (residue 4 = (*S,S*)H-Ala(αOH)). After a translational superposition of the centers of mass and rotational fit using the backbone atoms of residues 2–6, we calculated the pairwise distances based on the atom-positional RMSD of the backbone atoms (N, C, C_α, and C_β) of residues 2–6 for all structures in each of the data sets. These distance matrices were further analyzed using the density based common-nearerst-neighbor-cluster algorithm[8] to identify the fraction of the folded state in the various data sets. We used the following parameters for the clustering: β-heptapeptide A: nndc = 0.038 nm, nnnc = 10, perturbations to β-heptapeptide B: nndc = 0.030 nm, nnnc = 2, perturbations to β-heptapeptide C: nndc = 0.025 nm, nnnc = 2, perturbations to β-heptapeptide D: nndc = 0.030 nm, nnnc = 3 (λ = 0.25) and nndc = 0.030 nm, nnnc = 2 (other λ-values) *(S,S)*-configured β-heptapeptide E: nndc = 0.030 nm, nnnc = 2 and *(S,S)*-configured β-heptapeptide E: nndc = 0.030 nm, nnnc = 2. The cluster parameters were chosen according to the procedure described in ref. 8, which ensures that the cluster results are rather insensitive to a variation of the parameters.

RESULTS

Peptide A (residue 4 = (*S,S*)-β-HAla(αMe))

We calculated the normalized mutual information of all pairs of dihedral angles of peptide A in Figure 2 and found astonishingly small values. None of the NMI-values exceeded the threshold of 0.1, which means that the dihedral angles move largely independent of each other. For a lower threshold of 0.02, we obtained the mutual dependence graph, which is depicted in Figure 3. The dihedral angles χ_1 and χ_2 of each leucine side chain mutually influence each other but none of the side-chain dihedral angles is coupled to the backbone. In other words: the backbone conformation does not depend on the side-

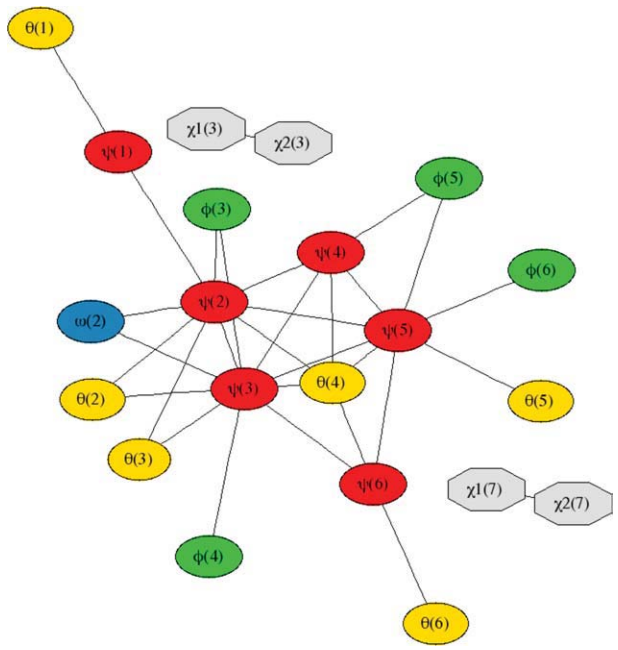

Figure 3

NMI-graph for peptide A, (*S,S*)-β-HAla(αMe), threshold: 0.02; blue: ω-dihedral angle ($C_\beta-C-N-C_\alpha$); green: ϕ-dihedral angle ($C-N-C_\alpha-C_\beta$); yellow: θ-dihedral angle ($N-C_\alpha-C_\beta-C$); red: ψ-dihedral angle ($C_\alpha-C_\beta-C-N$); grey: side-chain or endgroup dihedral angles. Residue sequence numbers are given between parentheses.

chain conformations. Instead, we find the ψ dihedral angles of residues 2–6 at the center of the graph. They obviously determine the backbone structure and - to a low degree – mutually depend on each other.

What determines the conformation of the backbone dihedral angles if it is not the conformation of the side chains? Figure 4 shows the backbone dihedral-angle distributions of peptide A sorted by the type of dihedral angle. The ω-dihedral angle is restricted to a maximum around 180° for all seven residues, which is expected as any other conformation would represent a torsion out of the corresponding peptide plane. Similarly, all ϕ- and θ-angles predominantly occupy one maximum: 240° for the ϕ-angles and ≈60° for the θ-angles. The only exception is the ϕ-angle in residue 1 in which the NH_3-group can rotate freely. This angle is omitted in Figure 4 for the sake of clarity. The ψ-dihedral-angle values show the largest variety of all backbone dihedral angles in molecule A and will therefore determine, which of the possible backbone conformations is assumed. This is also reflected in the average informational entropy of the dihedral angle distributions (see Fig. 5). The ω-dihedral angles have by far the lowest entropy, whereas the entropy of the ψ-dihedral angles is even slightly higher than those of the side-chain and endgroup dihedral angles. The entropy of the ϕ and θ dihedral angle distributions is significantly lower than those of the ψ dihedral angles. These differences in flexibility are not expected before, but we may hypothesize that the substituent on the C_β-atom on all seven residues sterically hinders the rotation around the adjacent bonds (ϕ and θ dihedral angles) leaving only the bond between the C_α- and the carbonyl-carbon to rotate relatively freely (ψ dihedral angle).

Figure 6 shows the ψ dihedral angle distributions of molecule A sorted by the type of residue. This graph illustrates three points. First, the ψ dihedral angles seem to visit the same four maxima (maximum I: 0–120°, maximum II: 120–180°, maximum III: 180–240° and, maximum IV: 240–360°), albeit with varying relative probability. This means that the generic shape of the dihedral-angle distribution is the same for all ψ-angles in molecule A and only the relative heights of the maxima and heights of the barriers vary. Second, the dihedral-angle distributions differ significantly even for residues with the same substituent. The amino acid type can therefore, contrary to intuition, not be the dominant fac-

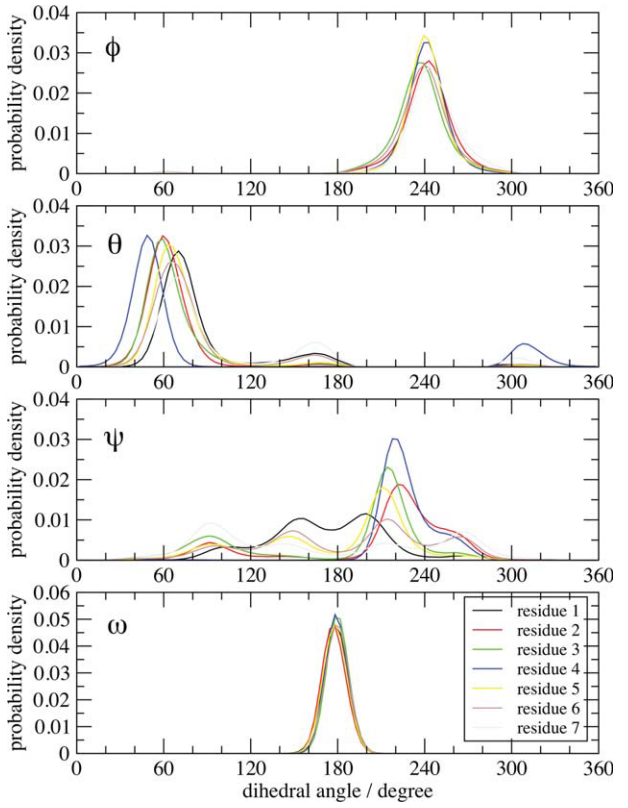

Figure 4

Distributions of the backbone-dihedral angles of H_2^+-β-HVal-β-HAla-β-HLeu-(*S,S*)-β-HAla(αMe)-β-HVal-β-HAla-β-HLeu-OH, panel ϕ: ϕ-dihedral angles = $C-N-C_\beta-C_\alpha$-dihedral-angles, panel θ: θ-dihedral angles = $N-C_\beta-C_\alpha-C$-dihedral-angles, panel ψ: ψ-dihedral angles = $C_\beta-C_\alpha-C-N$-dihedral-angles, panel ω: ω-dihedral angles = $C_\alpha-C-N-C_\beta$-dihedral-angles, *black*: residue 1, *red*: residue 2, *green*: residue 3, *blue*: residue 4, *yellow*: residue 5, *brown*: residue 6, *grey*: residue 7, sampling error negligible (error bars not shown).

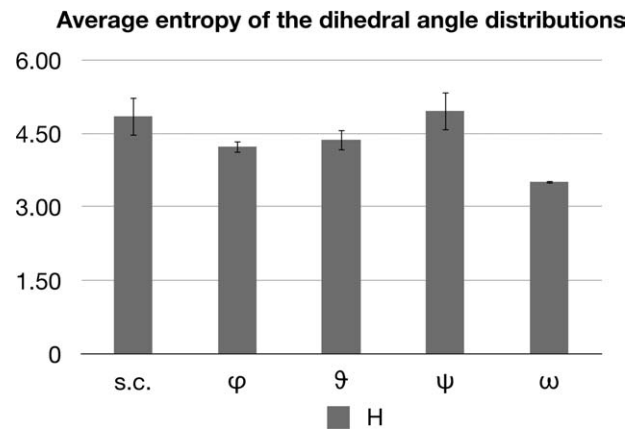

Figure 5

Entropy of the dihedral-angle distributions of peptide A, H_2^+-β-HVal-β-HAla-β-HLeu-(*S,S*)-β-HAla(αMe)-β-HVal-β-HAla-β-HLeu-OH, sorted by type, s.c.: side chain and endgroup dihedral angles. The values are averages of over 6 (ϕ, ψ, ω), 7 (θ) and 9 (s.c.) dihedral angles, the error bars show the standard deviation of the data set.

tor for the relative probability densities of the different backbone conformations. Third, the ψ-angle of residue 4 is the only ψ-angle, which predominantly populates a single maximum (maximum III). Note that residue 4 is also the only residue, which has a substituent on the C_α-atom – a fact supporting the hypothesis that substituents sterically hinder the rotation around the adjacent bonds.

Model for the conformational distribution of peptide A

In summary, these observations suggest the following model of the relative population of the conformations of molecule A.

- The side chains move freely. Their conformations and the conformations of the backbone are independent of each other.
- On all residues, the C_β-substituents sterically restrict the ϕ- and θ-dihedral angles to essentially one conformation.
- The two S-configured substituents on residue 4 sterically restrict the ψ-angle to (essentially) maximum III of the ψ-dihedral angle distribution, which is the conformation it would assume in a 3_{14}-helix.
- Confined to only one conformation residue 4 acts as primer for hydrogen bonds to the neighboring residues and thus enhances the probability of the 3_{14}-helix.
- The relative populations of maxima I–IV of the distributions of the other six ψ-dihedral angles is distorted (if not dominated) by this primer.

To test this model, we perturbed the substituents on residue 4 in molecule A into dummy atoms using using a λ-dependent Hamiltonian and the following three perturbation protocols:

- X=(*S,S*)-β-HAla(αMe) → X=(*S,S*)-β-HDum(αMe); λ = 0.25, 0.50, 0.75, 1.00
- X=(*S,S*)-β-HAla(αMe) → X=(*S,S*)-β-HAla(αDum); λ = 0.25, 0.50, 0.75, 1.00
- X=(*S,S*)-β-HAla(αMe) → X=(*S,S*)-β-HDum(αDum); λ = 0.25, 0.50, 0.75, 1.00

Here, Dum denotes a dummy atom, that is, an atom, which has no nonbonded interactions. For each value of λ, we evaluated the backbone dihedral-angle distributions, the fraction of the folded state in the complete ensemble and the hydrogen-bond pattern. At the end points, λ = 1.00, we additionally calculated the normalized mutual information between all dihedral angles.

Perturbations of peptide A to peptides B, C, and D

As in molecule A, all NMI between pairs of dihedral angles of the virtual molecules B–D were below the

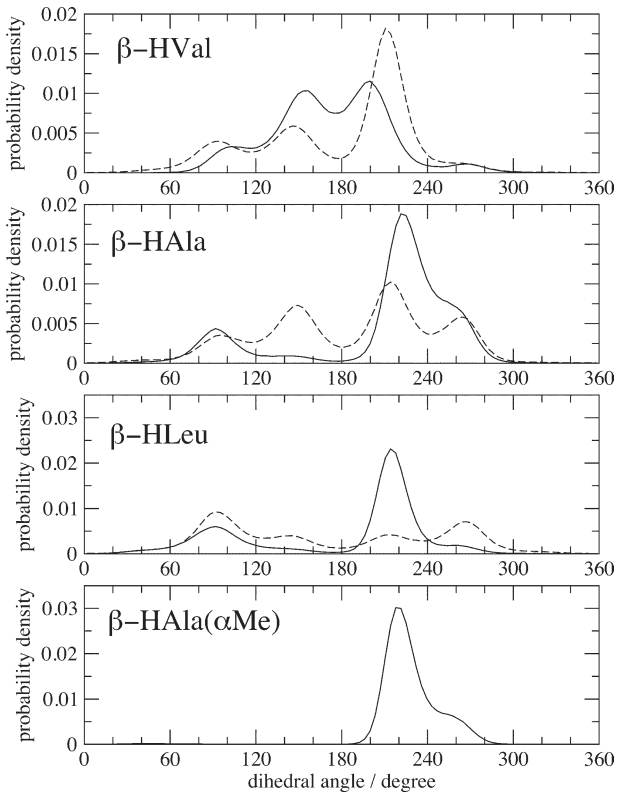

Figure 6

Distributions of the ψ dihedral angles of peptide A, H_2^+-β-HVal-β-HAla-β-HLeu-(*S,S*)-β-HAla(αMe)-β-HVal-β-HAla-β-HLeu-OH, sorted by type of residue. panel β-HVal: *solid*=residue 1, *dashed*=residue 5, panel β-HAla: *solid*=residue 2, *dashed*=residue 6, panel β-HLeu: *solid*=residue 3, *dashed*=residue 7, panel β-HAla(αMe): *solid*=residue 4, sampling error negligible (error bars not shown).

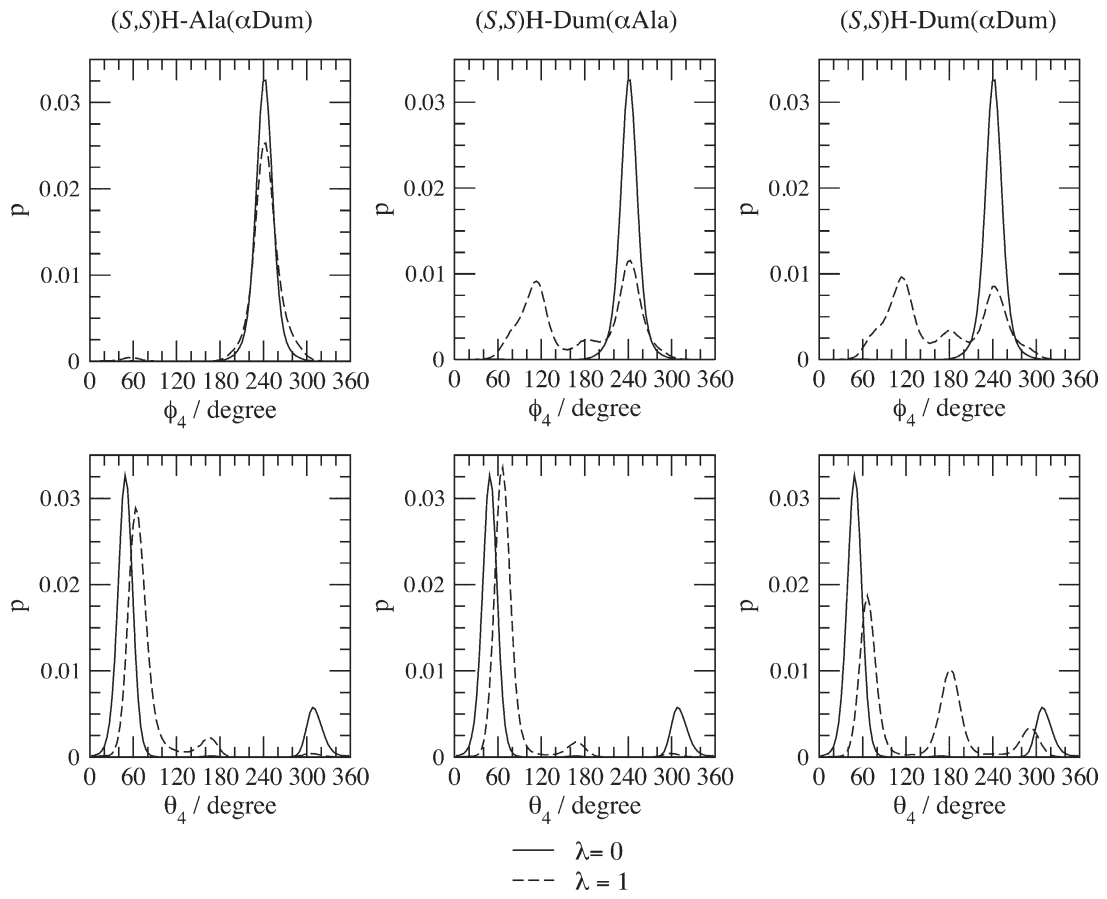

Figure 7

ϕ_4 and θ_4-dihedral angle distributions for the three perturbations. column 1: (*S,S*)H-Ala(αMe) → (*S,S*)H-Ala(αDum); column 2: (*S,S*)H-Ala(αMe) → (*S,S*)H-Dum(αMe); column 3: (*S,S*)H-Ala(αMe) →(*S,S*)H-Dum(αDum); *solid line:* $\lambda = 0$; *dashed line:* $\lambda = 1$; sampling error negligible (error bars not shown).

threshold of 0.1. Mutual dependence graphs for NMI $\geq$ 0.02 are reported in Figures S1–S3 of Supporting Information.[24] Compared with Figure 3, the pattern of mutual dependences is more complex and the number of mutual dependences with NMI $\geq$ 0.02 is greater in all three cases. We also find that the valine side chains are coupled to the adjacent backbone dihedral angles. But the general picture remains unchanged: at the center of the graphs, we find the ψ dihedral angles, which are coupled among each other and to the ϕ and θ dihedral angles. The conformation of the side-chain dihedral angles has no (leucine) or very little (valine) influence on the backbone dihedral angles.

In all three perturbations, the distributions of the ω, ϕ, and θ dihedral angles in residues 1–3 and 5–7 were virtually unaffected by the removal of the side chains in residue 4 (data shown in Supporting Information B–D[24]). In residue 4, the distribution of the ω dihedral angle (peptide plane) remained unchanged upon removal of the methyl-groups. The distributions of ϕ_4 and θ_4 for the end states of the three perturbations are depicted in Figure 7 (dashed line) and compared with those of peptide A (solid line). The removal of the methyl-group from the C_α-atom, – the steric block on the C_β-atom still being intact, does not cause a relevant change in either of the two distributions (column 1 of Fig. 7). If we on the other hand remove the methyl-group from the C_β-atom and leave the steric block on the C_α intact, ϕ_4 visits several maxima and the probability that it occupies the folded conformation is drastically decreased. The θ_4-distribution is still restricted to the maximum at 60° - obviously the rotation around the C_β-C_α-bond is hindered by the methyl-group on the C_α-atom (column 2 of Fig. 7). In the third perturbation both methyl-groups are removed and consequently both dihedral angles visit several maxima and the probability of finding them in the folded conformation is strongly decreased (column 3 of Fig. 7). From this we can conclude that the S-configured substituents on the C_β-atoms of all seven residues in peptide A act as steric blocks, which restrain the adjacent dihedral angles, ϕ and θ, to the folded conformation.

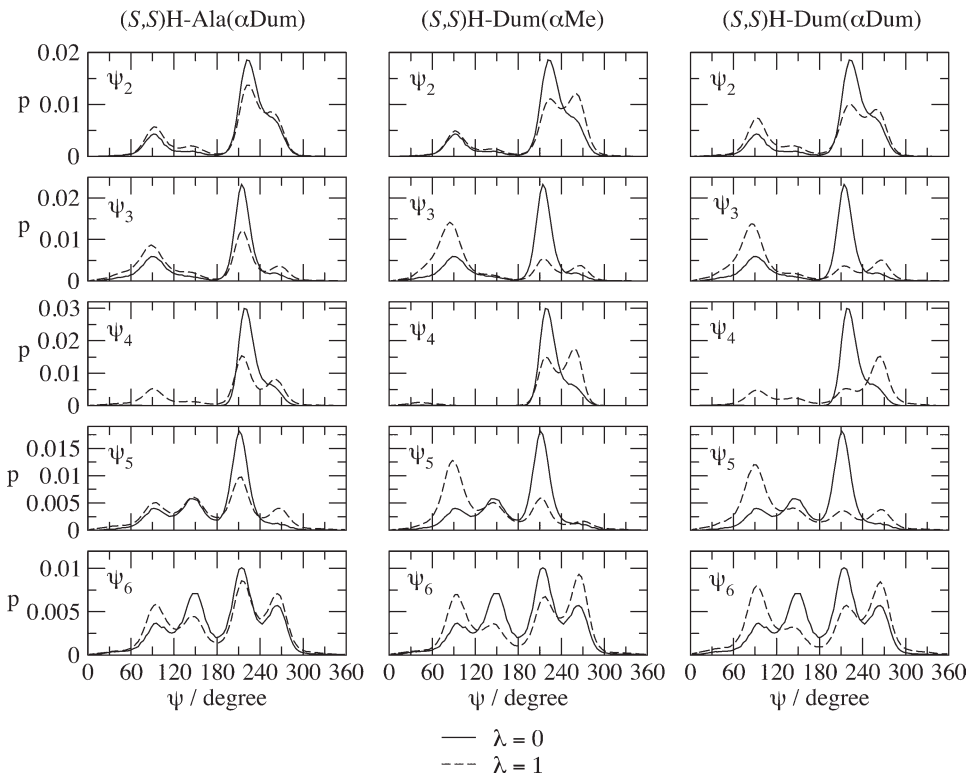

Figure 8

ψ-dihedral angle distributions of residues 2–6 for the three perturbations. column 1: (*S,S*)H-Ala(αMe) → (*S,S*)H-Ala(αDum); column 2: (*S,S*)H-Ala(αMe) → (*S,S*)H-Dum(αMe); column 3: (*S,S*)H-Ala(αMe) → (*S,S*)H-Dum(αDum); *solid line:* λ = 0; *dashed line:* λ = 1; sampling error negligible (error bars not shown).

All three perturbations had a strong effect on the conformations of the ψ-dihedral angles of the central residues (2–6). Their distributions are shown in Figure 8 (dashed lines) and compared with the corresponding distributions in peptide A (solid lines). This is in line with the finding that the ψ-dihedral angles mutually influence each other (Fig. 3), that is, a change in residue 4 will be transmitted to other residues via the ψ-dihedral angle conformations. If the methyl-group on the C_β-atom (which is not adjacent to the ψ-dihedral angle) is removed, the sequence of probabilities with which each of the ψ-dihedral angles visits the four maxima is retained. However, the probability of finding ψ_3 to ψ_5 in the folded conformation is noticeably decreased and ψ_4 additionally visits maximum I. If we remove the methyl-group on the C_α-atom, the folded conformation (maximum III) is no longer the most likely conformation of any of the ψ-dihedral angles of residues 2–6. Instead ψ_2 and ψ_4 visit maximum IV with a slightly higher probability than maximum III and for residue 3, 5, and 6, we even see a a complete inversion of the relative populations: maximum I (residue 3 and 5) and maximum IV (residue 6) become the most likely conformations. If both methyl groups are removed, ψ_4 samples all four maxima and the probability of finding it in maximum III is drastically decreased. The ψ-distributions of the other residues have similar features as in the second perturbation.

The hypothesis that residue 4 acts as primer, which once it is in the folded conformation, causes the rest of the peptide to fold cooperatively, is tested in Figure 9. Here we present conditional ψ-distributions of the central residues and compare them to the corresponding ψ-distributions of peptide A (black lines). Red lines correspond to the distribution of ψ-dihedral angles given that ψ_4 is in the folded conformation (maximum III) and blue lines correspond to the inverse situation: the ψ-dihedral angle distributions given that ψ_4 is not in maximum III. Their weighted sum returns the complete distribution, which was depicted in Figure 8. We expect that the ψ-distributions if ψ_4 is in maximum III (red lines), parallel those of peptide A in which ψ_4 is sterically restricted to maximum III, whereas the complementary curves account for the differences we see in the complete distributions. This expectation is completely met for the first perturbation in which the end state corresponds to an all β^3-substituted heptapeptide, and it is largely fulfilled for the second perturbation. If both methyl groups

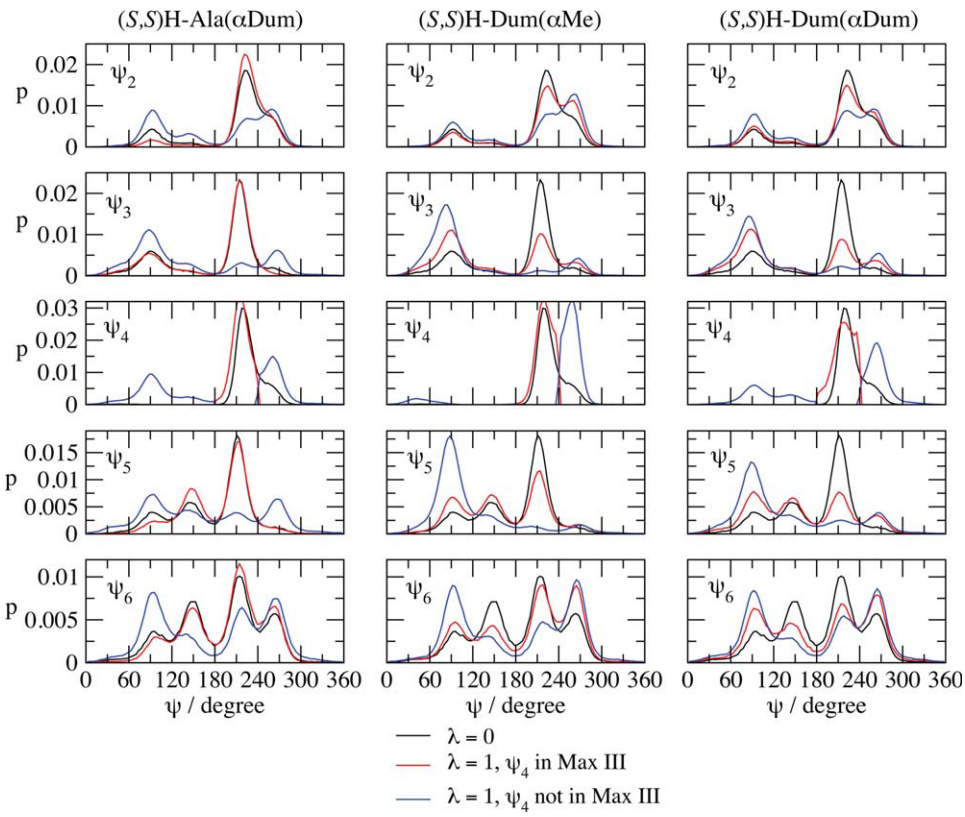

Figure 9

ψ-dihedral angle distributions of residues 2–6 for the three perturbations. column 1: (*S,S*)H-Ala(αMe) → (*S,S*)H-Ala(αDum); column 2: (*S,S*)H-Ala(αMe) → (*S,S*)H-Dum(αMe); column 3: (*S,S*)H-Ala(αMe) →(*S,S*)H-Dum(αDum); *black line:* λ = 0; *red line:* λ = 1, ψ_4 in maximum III; *blue line:* λ = 1, ψ_4 not in maximum III; sampling error negligible (error bars not shown).

are removed, the general trend is still visible but the peptide has become so flexible that the conformation of the central residue does not play a dominant role anymore.

In Table II we test whether the above analysis of dihedral-angle distributions is also reflected in more direct descriptors of the folded state. We look at the occurrence of the folded state as identified by a density-based cluster analysis and the occurrence of 3_{14}-helical hydrogen bonds. The cluster analysis shows that if the methyl group on the C_α-atom is removed, the fraction of the folded conformation in the entire ensemble decreases from about 60 to 37%. If the methyl group on the C_β-atom is removed the relative probability of the folded conformation is decreased far more drastically: only 5% of the ensemble is still folded. Note that for about half of the ensemble ψ_4 still is in maximum III (folded conformation, Fig. 8) but because of the mutual dependence of the ψ-dihedral angles, the destabilization of the folded state spreads in a nonlinear fashion. This effect is even

Table II

Occurrence (in %) of the 3_{14}-Helical Conformation (as Identified by Density based Clustering) and 3_{14}-Helical Hydrogen Bonds in the Trajectories

	*(S,S)*HAla(αMe)	→ *(S,S)*HAla(αDum)				→ *(S,S)*HDum(αMe)				→ *(S,S)*HDum(αDum)					
H-bond	λ = 0	0.25	0.50	0.75	1.00	0.25	0.50	0.75	1.00	0.25	0.50	0.75	1.00	*(S,S)*HAla(αF)	*(S,S)*HAla(αOH)
3_{14}-helix	60	62	30	19	37	43	28	24	5	59	36	18	(5)	52	30
NH(1)—O(3)	18	19	17	16	14	17	16	15	12	20	15	11	8	16	14
NH(2)—O(4)	53	53	24	17	34	37	26	23	10	51	32	16	6	44	27
NH(3)—O(5)	62	58	29	18	35	43	30	26	11	56	37	18	6	47	29
NH(4)—O(6)	55	49	26	19	24	39	22	18	10	49	29	13	4	41	27
NH(5)—O(7)	16	16	10	9	11	13	8	9	4	16	10	5	2	11	9
NH(5)—OH(7)	6	6	5	3	6	6	3	4	1	6	2	1	1	2	2

The number in brackets denotes a cluster which is predominantly helical but the borders of which are not as crisp as for the other helical clusters.

greater if both methyl groups are removed. The results of the hydrogen-bond analysis parallel those of the cluster analysis.

Peptides E and F

To test the model for the conformational distributions of β^3-peptides, we analyzed simulations of peptides E and F, which differ from peptide A only in the C_α-substituent on residue 4.

The mutual-information graphs of the C^{Si} substituted peptides E and F (Figs. S4 and S5 of Supporting Information[24]) show more and also slightly stronger mutual dependences with NMI > 0.02 than that of peptide A but the main features of the graphs are the same as for peptide A. The ψ-dihedral angles are at the center of the graph and the side chains are not or only loosely coupled to the backbone (cf. Supporting Information A[24]). The available simulation data did not suffice for the calculation of the mutual-information of the C^{Re} substituted peptides E and F.

Independent of whether residue 4 bears a fluoro- or a hydroxy-substituent and independent of the configuration of this substituent, the distributions of all ω-, ϕ-, and θ-dihedral angles do not differ greatly from those of peptide A (cf. Supporting Information E). This supports the idea that the mere existence of a substitute on the C_β-atoms dominates the distributions on the adjacent backbone dihedral angles. The ψ-dihedral angle distributions, however, were influenced by the different substituents and are depicted in Figure 10.

The distributions of both C^{Si} substituted peptides show the same features as the corresponding distributions of peptide A, endorsing that the substitution pattern plays a dominant role in stabilizing the folded structure. A closer look, however, shows that the probabilities of the maximum, which corresponds to the folded structure (maximum III) for the hydroxy-substituted peptide F are decreased with respect to those of peptide A. The ψ-distributions of peptide E, despite the fact that fluorine is significantly smaller than a methyl group, are almost equal to those of peptide A. Obviously, electrostatic effects come into play and one may speculate about the reasons for this. In the case of peptide F, the unfolded structures might be stabilized by intramolecular hydrogen bonds and the fluoro-substituent on peptide E might artificially increase its bulkiness by tight interactions with the surrounding solvent molecules. The cluster analysis and the hydrogen-bond analysis (Table II) confirm the results of the dihedral-angle distribution. Peptide E is about 50% folded whereas in peptide F the occurrence of the folded conformation is reduced to about 30%.

The ψ_4-distributions of the C^{Re} substituted peptides E and F differ greatly from that of peptide A: They are not restrained to maximum III but cover all four maxima. The fourth residue, therefore, cannot act as a primer to folding and consequently the distributions of ψ_2, ψ_3, ψ_5, and ψ_6 do not resemble their counter parts in peptide A, but are rather similar to those of peptide D (no substituents on residue 4).

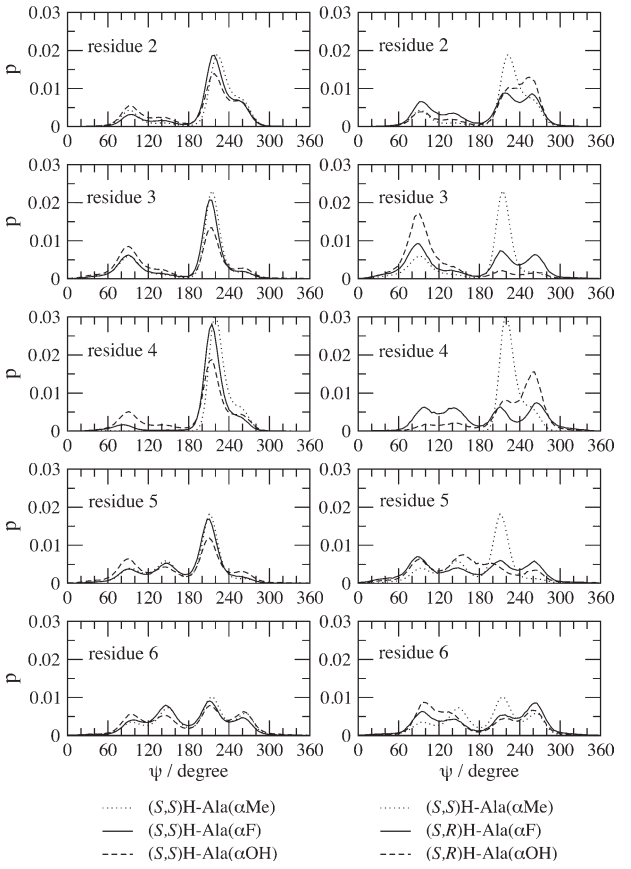

Figure 10

ψ-dihedral-angle distributions (C—N—C_α—C_β) for peptide E (residue 4=(*S*,*S*)-β-HAla(αF) and residue 4=(*S*,*R*)-β-HAla(αF)) and peptide F (residue 4=(*S*,*S*)-β-HAla(αOH) and residue 4=(*S*,*R*)-β-HAla(αOH)) compared to the corresponding distributions of peptide A; sampling error negligible (error bars not shown).

DISCUSSION

We have devised and tested a model for the conformational distribution of β-peptides with aliphatic residues by carefully analyzing the mutual dependences between dihedral angles and dihedral-angle distributions.

The mutual information graphs reveal that the particular conformation of the side chain has no influence on the backbone structure. Pictorially spoken: the backbone does not see what the side chains are doing. Likewise the type of the side chain does not play a decisive role for the stabilization of the folded conformation, because different residues with the same side chain show different ψ-dihedral-angle distributions, as we could show by comparing the backbone dihedral angle distributions of

amino acids with the same residue. It is rather the substitution pattern that determines the backbone conformation. We could show that in β^3-substituted residues the backbone dihedral angles adjacent to the side chain, ϕ and θ, are restricted in the folded conformation. The relative probability of the folded conformation is in these cases increased by sterically excluding large parts of the unfolded conformational space. This is in line with the finding that β^3-substituted β-peptides form stable 3_{14}-helices[3,6] and that residues branched at the first carbon atom, that is, which are bulky at a position close to the backbone, promote helicity.

The ψ-dihedral angles are consequently the only flexible degrees of freedom – their conformation determines the backbone structure. If the ψ-angle of the central residue is additionally restricted to the folded conformation, this residue acts as primer around that the neighboring residues fold. We could pinpoint this effect by perturbing the methyl groups on residue of 4 in peptide A to dummy atoms. The increased flexibility of ψ_4 spread via the other ψ-dihedral angles throughout the molecule.

Comparison to α-peptide folding

Compared to α-peptides in water, β-peptides in methanol form remarkably stable helices - even if the chain length is very short (less than 30 backbone dihedral angles). One reason for this might be the properties of the solvent: water molecules are capable of forming stronger hydrogen bonds with the backbone of a peptide than methanol molecules, which increases the relative stability the unfolded conformations. Indeed, one finds that β-peptides of similar length form less stable 3_{14}-helices in water than in methanol.[25] However, one also finds that neither in water nor in methanol, short α-peptides fold into stable helices, even when their conformational space is restricted by an aminoisobutyric-acid moiety (Aib).[26] So, the question remains: "How do the structural features of β-peptides stabilize the folded conformation?"

In the following discussion, we compare β-peptides with $3n$ residues to α-peptides with $4n$ residues. This choice of the number of residues ensures that both types of peptides have the same number of backbone dihedral angles: $12n$. The equilibrium constant of the folding-unfolding equilibrium K is given by the free-energy difference between the folded and the unfolded state $\Delta G = G_{\text{folded}} - G_{\text{unfolded}}$

$$K = \exp\left(-\frac{\Delta G}{RT}\right) = \exp\left(-\frac{\Delta H}{RT}\right)\exp\left(\frac{\Delta S}{R}\right), \qquad (7)$$

where R is the gas constant, T the absolute temperature, ΔH the enthalpy difference, ΔS the entropy difference. We have used $\Delta G = \Delta H - T\Delta S$. We expect that the enthalpy difference ΔH for β-peptides is about the same or somewhat smaller than that for α-peptides of the same backbone length, because both helices are mainly stabilized by intramolecular hydrogen bonds. α-Peptides, however, have more peptide planes per backbone length, and therefore, for a given chain length, form more intramolecular hydrogen bonds and additionally, α-helices are typically stabilized by favorable side-chain–side-chain interactions. Hence:

$$\Delta H(\beta, 3n \text{ residues}) \geq \Delta H(\alpha, 4n \text{ residues}) \qquad (8)$$

Consequently, the stability of 3_{14}-helices must be caused by an entropic effect. Naively one would, however, expect a destabilizing entropic effect, because β-peptides have three flexible dihedral angles per residue whereas α-peptides only have two. With only one in four backbone dihedral angles being rigid (peptide plane), a β-peptide could explore many more conformations than a comparable α-peptide, which increases the entropy of the ensemble of its unfolded conformations or - formulated differently - decreases the relative probability of its folded conformation. With ΔH equal or bigger and ΔS smaller than in α-peptides, one would not expect that β-peptides form stable structures.

A closer look at the dihedral-angle distributions resolves this contradiction. As shown in this contribution, the ϕ- and θ-dihedral angles of β^3-substituted β-peptides populate only one maximum, that is, these dihedral angles are quasi-rigid, leaving only the ψ-dihedral angle as an flexible dihedral angle. Hence, in β^3-substituded β-peptides only one in four dihedral angles is flexible. In α-peptides, on the other hand, the ϕ-dihedral angles is quasi-rigid and the ψ-dihedral angle flexible, adding up to one flexible dihedral angle in three. From this we can conclude that accessible unfolded conformational space of β-peptides with a C^{Si} configured substitute on the C_β-atom is smaller than that of comparable α-peptides and hence,

$$\Delta S(\beta, 3n \text{ residues}) > \Delta S(\alpha, 4n \text{ residues}). \qquad (9)$$

This is in agreement with the earlier finding that the accurate description of (the unexpectedly small) unfolded conformational space is essential for the modeling of (β-) peptide folding equilibria.[27]

There are two ways in which the steric block exerted by the β^3-substituents could influence the conformational ensemble of β-peptides: (i) steric clashes could destabilize a certain conformation, thereby changing ΔH and consequently also the equilibrium constant between this conformation and the rest of the ensemble; (ii) the dihedral angles could be kinetically trapped in one conformation. Figure 11 illustrates the factors that influence the rate constants of the transition between two states, a folded one f and an unfolded one u, and that could cause a kinetic trap. According to Kramers' theory, the rate constant of unfolding (in Fig. 11) is given as

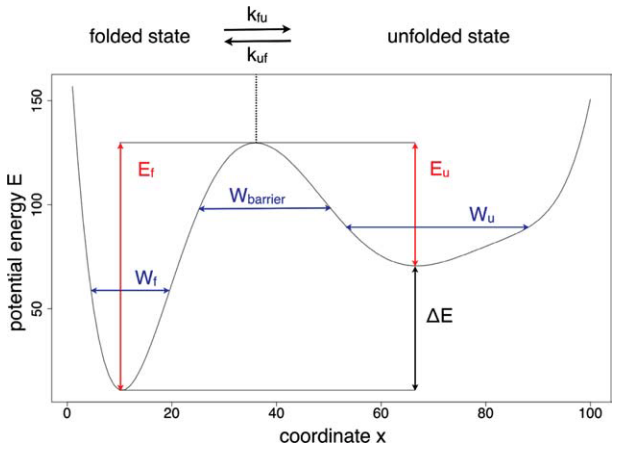

Figure 11

Potential energy surface for a 2-state model of the peptide folding equilibrium.

$$k_{fu} = \frac{m\omega_{\text{barrier}}}{\zeta} \cdot \frac{\omega_f}{2\pi} \cdot \exp\left(-\frac{E_f}{k_B T}\right) \qquad (10)$$

The third factor denotes the probability of reaching the transition state and is a function of the barrier height E_f. (k_B is the Boltzmann constant and T the absolute temperature.) The second factor corresponds to the frequency with which an attempt to reach the transition state is made and is proportional to the frequency ω_f, which is associated with the (harmonically approximated) potential energy function of state f. The broader the width of this well (W_f in Fig. 11), the lower the frequency ω_f. And finally, the first factor corresponds to the fraction of "productive trajectories," that is, from all systems that reach the transition state the fraction of those that actually cross into state u and do not get pushed back to state f. In Kramers' theory, this factor is modeled as diffusion across the barrier where ω_{barrier} is the frequency, which is associated with the (harmonically approximated) potential energy function of the barrier, m is the mass of the particle and ζ the friction coefficient. The wider the barrier (W_{barrier} in Fig. 11), the lower the fraction of "productive trajectories." In this framework, a kinetic trap can be caused by (i) a high barrier (E_f), (ii) a broad well in state f(W_f), or (iii) a wide barrier (W_{barrier}). Considering that the dihedral angles move largely independent of each other and are bound degrees of freedom (i.e., neither the width of the barrier nor the width of the potential well can be arbitrarily large), it is hardly conceivable that a kinetic trap might be caused by the second or third effect. In summary, the rotation around the ϕ- and θ-dihedral angles in β^3-peptides is restricted to one maximum by a steric clash, which either destabilizes all other conformational maxima, or which causes a kinetic trap by inducing high rotational barriers around this maximum. The data presented in this contribution does not allow a clear conclusion as to which of the two effects causes the observed block. Note, however, that for a kinetic trap from which the system cannot escape even on experimental time scales the allowed region has to be surrounded by barriers with heights of several tens of kJ/mol.

Likewise, no unambiguous conclusion as to what causes the steric clash can be drawn from the presented data. However, from Ramachandran plots of α-peptides it is known that the steric interaction of the side chain with the carbonyl atom of the preceding peptide group restricts the ϕ-dihedral angle adjacent to the side chain to about 270°. In α-peptides, the first atom of the side chain is separated by four bonds from the carbonyl oxygen of the preceding peptide group. This is also the case in β^3-peptides and hence the ϕ-dihedral angles of β^3-peptides are likely to be restricted via the same mechanism. Additionally, the first atom of a β^3-side chain is separated by four bonds from the carbonyl-oxygen of the following peptide group. The restriction of the θ-dihedral angles might therefore also be caused by this mechanism. According to this, β^2-peptides (in which the amino acids are substituted at the C_α atom leading to a distance of five bonds to the preceding peptide group and a distance of three bonds to the following peptide group) should not be stabilized by steric clashes, and therefore, form less stable helices. This presumption is supported by the experimental finding that the helical structure of β^2-peptides is only stable at −20°C.[28]

CONCLUSIONS

The folding of β-peptides is governed by different biophysical effects than that of natural peptides. The second carbon atom between the peptide planes allows the substitution pattern to be varied, a parameter which is not present in natural peptides, and leads to various "substitution classes" of β-peptides. Because of steric interactions of the side chains with the backbone, a given part of the conformational space might be accessible for one class of β-peptides but inaccessible for others. The class of β^3-substituted peptides investigated in this contribution folds into 3_{14}-helices. We could show that the size of the unfolded conformational space of these peptides is smaller than that of a comparable α-peptide and therefore the relative probability of the folded conformation is increased. The folded state of β^3-peptides is not stabilized by specific side-chain–side-chain interactions and hence also largely independent of the side-chain sequence. As a consequence, analogies between β-peptide folding and α-peptide folding should be handled with caution.

ACKNOWLEDGMENTS

Financial support by the National Centre of Competence in Research (NCCR) (Structural Biology) of the

Swiss National Science Foundation (SNSF) is gratefully acknowledged.

REFERENCES

1. Seebach D, Beck AK, Bierbaum DJ. The world of beta- and gamma-peptides comprised of homologated proteinogenic amino acids and other components. Chem Biodivers 2004;1:1111–1239.
2. van Gunsteren WF, Gattin Z. Simulation of Folding Equilibria. In: Hecht S, Huc I, editors. Foldamers: structure, properties and applications. Wiley-VCH Verlag GmbH & Co. KGaA Weinheim; 2007; pp 173–192.
3. Martinek TA, Fülöp F. Side-chain control of beta-peptide secondary structures - design principles. Euro J Biochem 2003;270:3657–3666.
4. Peter C, Rueping M, Wörner HJ, Jaun B, Seebach D, van Gunsteren WF. Molecular dynamics simulations of small peptides: can one derive conformational preferences from ROESY spectra? Chem-A Eur J 2003;9:5838–5849.
5. Seebach D, Ciceri PE, Overhand M, Jaun B, Rigo D, Oberer L, Hommel U, Amstutz R, Widmer H. Probing the helical secondary structure of short-chain beta-peptides. Helvetica Chimica Acta 1996;79:2043–2066.
6. Kritzer JA, Tirado-Rives J, Hart SA, Lear JD, Jorgensen WL, Schepartz A. Relationship between side chain structure and 14-helix stability of beta(3)-peptides in water. J Am Chem Soc 2005;127:167–178
7. Daura X, van Gunsteren WF, Rigo D, Jaun B, Seebach D. Studying the stability of a helical beta-heptapeptide by molecular dynamics simulations. Chem-A Eur J 1997;3:1410–1417.
8. Keller B, Daura X, van Gunsteren WF. Comparing geometric and kinetic cluster algorithms for molecular simulation data. J Chem Phys, in press.
9. van Gunsteren WF, Billeter SR, Eising AA, Hünenberger PH, Krüger P, Mark AE, Scott WRP, Tironi IG. Biomoleuclar simulation: the GROMOS96 manual and user guide: vdf Hochschulverlag AG an der ETH Zürich. 1996.
10. Daura X, Mark AE, van Gunsteren WF. Parametrization of aliphatic CH_n united atoms of GROMOS96 force fields. J Comput Chem 1998;19:535–547.
11. Boned R, van Gunsteren WF, Daura X. Estimating the temperature dependence of peptide folding entropies and free enthalpies from total energies in molecular dynamics simulations. Chem-A Eur J 2008;14:5039–5046.
12. Scott WRP, Hünenberger PH, Tironi IG, Mark AE, Billeter SR, Fennen J, Torda AE, Huber T, Krüger P, van Gunsteren WF. The GROMOS biomolecular simulation program package. J Phys Chem A 1999;103:3596–3607.
13. Ryckaert JP, Ciccotti G, Berendsen HJC. Numerical-integration of Cartesian equations of motion of a system with constraints - molecular-dynamics of n-alkanes. J Comput Phys 1977;23:327–341.
14. Berendsen HJC, Postma JPM, van Gunsteren WF, Di Nola A, Haak JR. Molecular-dynamics with coupling to an external bath. J Chem Phys 1984;81:3684–3690.
15. Barker JA, Watts RO. Monte Carlo studies of the dielectric properties of water-like models. Mol Phys 1973;26:789–792.
16. Tironi IG, Sperb R, Smith PE, van Gunsteren WF. A generalized reaction field method for molecular dynamics simulations. J Chem Phys 1995;102:5451–5459.
17. Beutler TC, Mark AE, Van Schaik RC, Gerber PR, van Gunsteren WF. Avoiding singularities and numerical instabilities in free-energy calculations based on molecular simulations. Chem Phys Lett 1994;222:529–539.
18. Christen M, Hünenberger PH, Bakowies D, Baron R, Bürgi R, Geerke DP, Heinz TN, Kastenholz MA, Kräutler V, Oostenbrink C, Peter C, Trzesniak D, van Gunsteren WF. The GROMOS software for biomolecular simulation: GROMOS05. J Comput Chem 2005; 26:1719–1751.
19. Schuler LD, Daura X, Van Gunsteren WF. An improved GROMOS96 force field for aliphatic hydrocarbons in the condensed phase. J Comput Chem 2001;22:1205–1218.
20. Walser R, Mark AE, van Gunsteren WF, Lauterbach M, Wipff G. The effect of force-field parameters on properties of liquids: parametrization of a simple three-site model for methanol. J Chem Phys 2000;112:10450–10459.
21. Gattin Z, Schwartz J, Mathad RI, Jaun B, van Gunsteren WF. Interpreting experimental data by using molecular simulation instead of model building. Chem-A Eur J 2009;15:6389–6398.
22. Gattin Z, van Gunsteren WF. Influence of backbone fluorine substitution upon the folding equilibrium of a beta-heptapeptide. J Phys Chem B 2009;113:8695–8703.
23. Noé F, Horenko I, Schütte C, Smith JC. Hierarchical analysis of conformational dynamics in biomolecules: transition networks of metastable states. J Chem Phys 2007;126:155102.
24. Supplementary material.
25. Cheng RP, Gellman SH, DeGrado WF. Beta-peptides: from structure to functions. Chem Rev 2001;101:3219–3232.
26. Soares T, Christen M, Hu K, van Gunsteren WF. Alpha- and beta-polypeptides show a different stability of helical secondary structure. Tetrahedron 2004;60:7775–7780.
27. van Gunsteren WF, Bürgi R, Peter C, Daura X. The key to solving the protein-folding problem lies in an accurate description of the denatured state. Angewandte Chemie-Int Ed 2001;40:351–355.
28. Lelais G, Seebach D. Beta(2)-amino acids - syntheses, occurrence in natural products, and components of beta-peptides. Biopolymers 2004;76:206–243.